ORIGINAL ARTICLE



Effects of machining gap on the surface integrity in CBN spherical magnetic abrasives grinding of ZrO₂ ceramic

Linzhi Jiang¹ · Tieyan Chang² · Guixiang Zhang¹ · Yu-Sheng Chen² · Xue Liu¹ · Haozhe Zhang¹

Received: 2 August 2023 / Accepted: 15 September 2023 / Published online: 23 September 2023 © The Author(s), under exclusive licence to Springer-Verlag London Ltd., part of Springer Nature 2023

Abstract

Due to the high hardness and brittleness of zirconia ceramic (ZrO₂), it is difficult to generate a good surface integrity by traditional grinding. The surface quality of ZrO₂ can be greatly improved by magnetic abrasive finishing (MAF) with spherical CBN/Fe-based magnetic abrasive particles (MAPs) prepared by gas atomization. In this study, it was found that the difference of machining gap in MAF would seriously affect the surface integrity of ZrO₂. The grinding pressure of CBN MAPs on ZrO₂ under different machining gaps was analyzed theoretically. The surface morphology, surface roughness Ra and material removal amount MR, grinding pressure, surface temperature and residual stress, subsurface damage and the morphology of MAPs adsorbed by magnetic pole after grinding were studied under different machining gaps (3 mm to 1 mm). The results show that when the machining gap is large, the grinding pressure is small, the number of MAPs involved in grinding is small, and the surface integrity of ZrO₂ do not change significantly. When the machining gap is small and the grinding pressure is too large, a large number of MAPs are extruded from the machining area, the magnetic abrasive brush is changed from flexible to rigid, and the ceramic surface is mainly removed by brittleness. After grinding, many cracks and pits are generated on the ceramic surface, and cracks are also produced on the subsurface, which destroys the surface integrity of the workpiece. Under the appropriate machining gap, it can not only ensure that the grinding pressure is large, but also make the ZrO₂ surface mainly plastic removal, and finally obtain the best surface integrity. The optimal machining gap in this experiment is 2 mm.

 $\textbf{Keywords} \ \ \text{Machining gap} \cdot \text{Surface integrity} \cdot \text{Magnetic abrasive finishing} \cdot \text{CBN spherical magnetic abrasive particles} \cdot \text{ZrO}_2 \ \text{ceramic}$

1 Introduction

As a typical high hardness and brittleness material, zirconia ceramic (ZrO₂) is widely used in aerospace and biomedical fields because of its low density, wear resistance, corrosion resistance and other characteristics [1–3]. With the development of science and technology, the requirements for its surface quality are increasingly high. At present, grinding is still the main processing method to improve their surface quality [4–7]. In the traditional grinding process, the surface of ZrO₂ is mainly removed by brittleness. Under the action

of large grinding force and grinding heat, a large number of pits and cracks will be generated on its surface and cause subsurface damage, which will seriously affect the surface quality and service life of ceramics [8–10]. Therefore, it is of great significance to study how to restrain machining damage and improve the surface integrity of ZrO₂.

In recent years, a lot of research has been done on how to improve the surface quality of ZrO_2 . Ma et al. developed a nontraditional hybrid laser-assisted grinding system combining laser and cubic boron nitride grinding wheel to cut and remove ZrO_2 surface through local laser heating and grinding wheel. Compared with conventional grinding, the surface integrity of ZrO_2 is significantly improved [11]. Liu et al. studied the effect of strain rate on grinding force, surface morphology and subsurface cracks when grinding ZrO_2 with diamond grinding wheel. The results show that increasing the grinding strain rate can effectively improve the grinding quality of ZrO_2 [12]. Zhang et al. designed a



[☐] Guixiang Zhang zhanggx2013@163.com

School of Mechanical Engineering, Shandong University of Technology, Zibo 255000, China

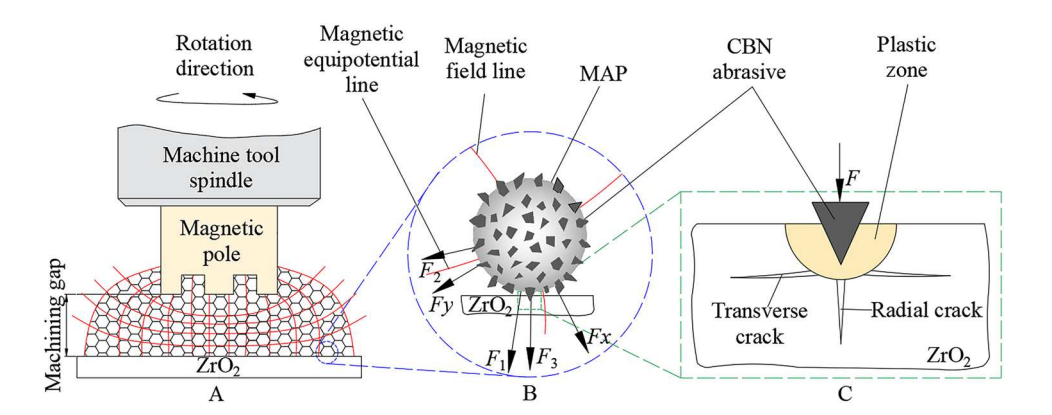
NSF's ChemMatCARS, The University of Chicago, Lemont, IL 60439, USA

type of the biomimetic fractal-branched grinding wheel based on leaf veins, which improves the coolant flow efficiency through the fractal structure of the wheel, so that it has better grinding performance than the original wheel [13]. Xiao et al. carried out experimental and theoretical research on the cutting force of ultrasonic vibration assisted side grinding of ZrO_2 , proposed a theoretical cutting force model, and determined the critical cutting depth of ductile-to-brittle transition [14]. At present, the grinding of ZrO_2 is mainly carried out with grinding wheel, which has large grinding force, high grinding temperature and is difficult to control the surface integrity.

Magnetic abrasive finishing (MAF) is a flexible machining technology that combines magnetic field and magnetic abrasive particles (MAPs). During the machining process, the grinding force on the workpiece is smaller than that of the grinding wheel, and the grinding heat generated is less [15–18]. It is very suitable for the plastic removal of micro-cutting of hard and brittle materials such as ZrO₂, and improving the surface integrity of ZrO₂. In the MAF of ZrO₂, Heng et al. studied the influence of magnetic pole shape and magnetic pole vibration frequency on the surface quality. Under the best grinding parameters, a high-quality ZrO₂ surface was obtained [19].

At present, studies on MAF of ZrO₂, especially on the ductile-to-brittle transition of ZrO₂ surface by MAF are rare. In MAF, we found that the change of machining gap is one of the most important factors that lead to the ductile-to-brittle transition on the surface of ZrO₂. The difference of machining gap seriously affects the surface integrity of ZrO₂. In order to reveal the effect of machining gap on surface integrity, this study analyzed the ductile-to-brittle transition, surface roughness and material removal amount, grinding pressure, surface temperature and residual stress, subsurface damage of ZrO₂ and the morphology of MAPs adsorbed by magnetic pole under different machining gaps. The research results provide experimental reference for MAF of hard and brittle ceramic materials, and also improve the surface integrity of ZrO₂.

Fig. 1 The schematic diagram of MAF of ZrO₂ surface with CBN spherical MAPs



2 Theoretical analysis

Figure 1 shows the schematic diagram of MAF of ZrO_2 surface with CBN spherical MAPs. When MAPs are filled in the magnetic field generated by the magnetic pole, the MAPs will be regularly arranged along the direction of the magnetic field, forming a flexible magnetic abrasive brush (Fig. 1A). The spindle of the machine tool drives the magnetic pole to rotate and move, and the MAPs absorbed by the magnetic pole grinds the surface of the workpiece. The effect of magnetic force on a single magnetic abrasive particle (MAP) is shown in Fig. 1B. In the magnetic field, MAP is mainly affected by the force F_x in the direction of the magnetic field line and the force F_y in the direction of the magnetic equipotential line. The combined force of the two is F_1 . Each force is shown in Eqs. (1) [20]:

$$\begin{cases} F_x = V \cdot X \cdot \mu_0 \cdot H \cdot \frac{\partial H}{\partial x} \\ F_y = V \cdot X \cdot \mu_0 \cdot H \frac{\partial H}{\partial y} \\ F_1 = \sqrt{F_x^2 + F_y^2} \end{cases}$$
 (1)

where V is the volume of MAP, X is the magnetic susceptibility of MAP, μ_0 is the vacuum permeability, H is the magnetic field strength at the location of MAP, $\partial H/\partial x$ and $\partial H/\partial y$ are the change rate of magnetic field intensity along the magnetic force line and magnetic equipotential line respectively.

When the magnetic abrasive brush is magnetized, the MAP will also be attracted by the surrounding MAPs. The magnetic attraction of a single MAP to a MAP is [21]:

$$F_i = 1.5\pi r^2 \mu_0 X_r^2 \frac{H^2}{3 + X_r^2} \tag{2}$$

where r is the radius of MAP. A single MAP will be subject to the magnetic attraction of multiple MAPs, and the combined traction force of multiple magnetic attractions is F_2 .

When the machining gap is gradually reduced, the magnetic abrasive brush will gradually change from flexible to rigid, and the MAPs will begin to be squeezed by the



machine tool spindle. The resultant force of the extrusion of a single MAP by surrounding MAPs is F_3 . With the reduction of machining gap, the rigidity of the magnetic abrasive brush increases. Consequently, the extrusion force of MAPs by surrounding MAPs also increases.

Therefore, within a certain range of machining gap, a single MAP in contact with the ZrO_2 surface will be affected by the magnetic force F_1 generated by the magnetic pole, the magnetic traction force F_2 and the extrusion force F_3 of the surrounding MAPs, and their normal forces are F_1 , F_2 and F_3 respectively. Then the downward grinding pressure F generated by a single MAP on the surface of ZrO_2 is:

$$F = F_1 \prime + F_2 \prime + F_3 \prime \tag{3}$$

It can be seen from Eqs. (1) and (2) that the magnetic force F_1 and the magnetic traction force F_2 are related to the magnetic field strength of the processing area where the MAP is located and the magnetic susceptibility of the MAP. Therefore, the force F_1 and F_2 can be changed by changing the magnetic field strength, which can be adjusted by the machining gap. The closer the region to the magnetic pole, the denser the magnetic induction lines, and the stronger the magnetic field strength. When the machining gap is large, the extrusion force F_3 is negligible, the grinding force of MAP on ceramic surface is generated by force F_1 and F_2 , which are small because of weak magnetic field strength in the processing area. With the reduction of machining gap, the increase of magnetic field strength leads to the increase of magnetic force F_1 and magnetic traction force F_2 , and the extrusion force F_3 begins to generate. The generation of grinding force is still dominated by force F_1 and F_2 . When the grinding gap is small enough, the magnetic abrasive brush changes from flexible to rigid, and the extrusion force F_3 becomes larger. Although the magnetic field strength further increases, the quantity of MAPs in the machining area is small, and the grinding pressure is mainly generated by the extrusion force F_3 .

The grinding removal methods of ZrO_2 are plastic removal and brittle removal, which are mainly related to the grinding pressure F. In MAF, the deformation and fracture diagram of CBN MAP on ZrO_2 is shown in Fig. 1C. Under the action of force F, the CBN abrasive will generate a plastic deformation zone on the surface of ZrO_2 , from which two main crack systems are generated: radial crack and transverse crack. Radial cracks usually lead to the reduction of material strength, while transverse cracks can cause the brittle removal of materials. The critical load F_R for generating radial cracks is [22]:

$$F_R = 54.5 \left(\alpha / \eta^2 \gamma^4 \right) \left(\frac{K_c^4}{H^3} \right) \tag{4}$$

where α , η and γ are constants, Kc is the fracture toughness of the ceramic material, and H is the hardness of the ceramic material. When $F > F_R$, radial cracks will be generated. Transverse cracks are usually generated when the pressure load is unloaded. The critical load F_T for transverse cracks can be expressed as [23]:

$$F_T = \delta \binom{K_c^4}{H^3} f \binom{E}{H} \tag{5}$$

where δ is a dimensionless constant, and f(E/H) is an attenuation function, $\delta f(E/H) \approx 2 \times 10^5$. When $F > F_T$, transverse cracks are generated, and the ceramic material is mainly removed by brittleness.

3 Experimental

3.1 Materials

As a machining tool in MAF, the performance of MAPs plays a crucial role in the surface integrity of the workpiece. The advantage of MAF lies in the flexibility and adaptability of MAPs during the machining process. Therefore, the ideal MAP shape should be spherical (Fig. 2). And the spherical MAP can achieve uniform distribution and maximum amount of ceramic abrasives on the surface of the iron substrate, resulting in higher machining efficiency and better machining uniformity in MAF. The machining tool used in this experiment is a new type of CBN/Fe-based spherical MAPs prepared by gas atomization (Fig. 3). It can be seen that the MAP has a good sphericity, and the CBN abrasives are uniformly and densely distributed on the surface of the iron substrate, which is basically consistent with the ideal MAP. The workpiece to be processed in this study is zirconia

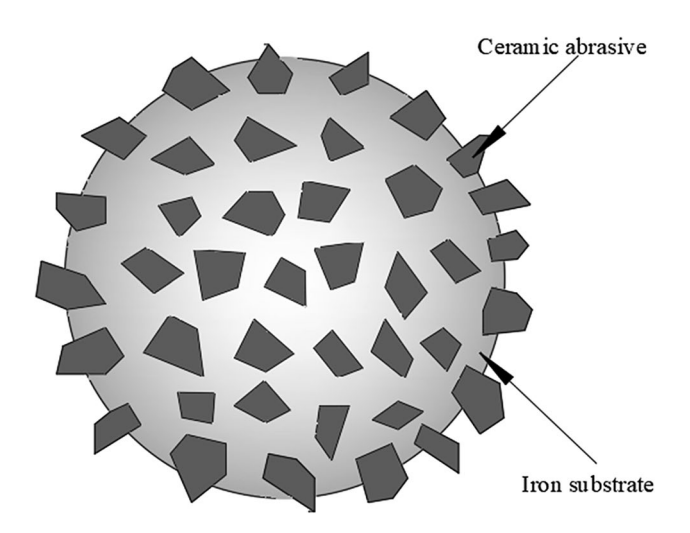


Fig. 2 Ideal model of MAP



Table 1 Magnetic abrasive finishing experimental parameters

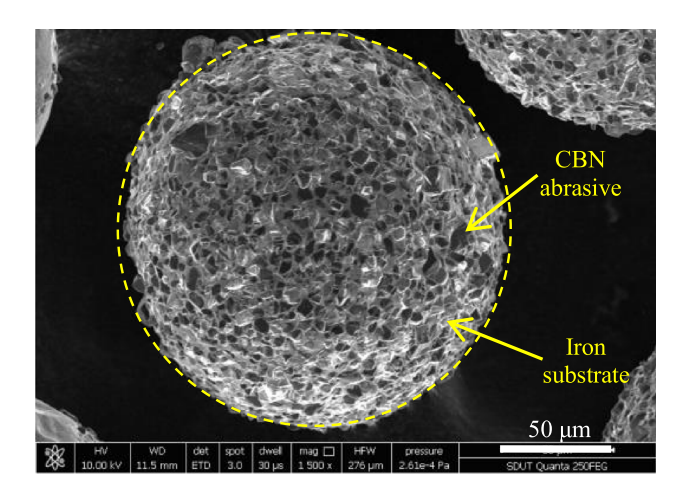


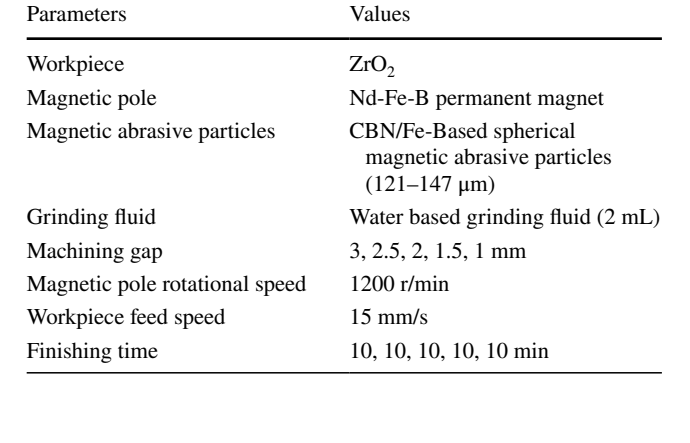
Fig. 3 CBN spherical MAPs prepared by gas atomization

ceramic, with a size of $40 \text{ mm} \times 40 \text{ mm} \times 2 \text{ mm}$ and an average initial roughness Ra of $0.37 \mu \text{m}$.

3.2 Experimental setup and conditions

The MAF device is modified from the XK7136C CNC machine tool, and the independently developed Nd-Fe-B slotted permanent magnetic pole is installed on the machine tool spindle (Fig. 4). During the experiment, it was found that changing the machining gap between the magnetic pole and the workpiece would have a significant impact on the surface quality of the workpiece, while other grinding parameters remained unchanged. Therefore, research was conducted on the impact of machining gap on the surface integrity of ZrO₂ ground with CBN MAPs. A total of five experiments were conducted, with machining gaps decreasing from 3 to 1 mm with 0.5 mm interval. The grinding time for each group of experiment was 10 min. It was found that surface integrity parameters such as surface morphology and surface roughness basically no longer changed after 10 min of grinding. The specific grinding parameters are shown in Table 1.

Fig. 4 Magnetic abrasive finishing device



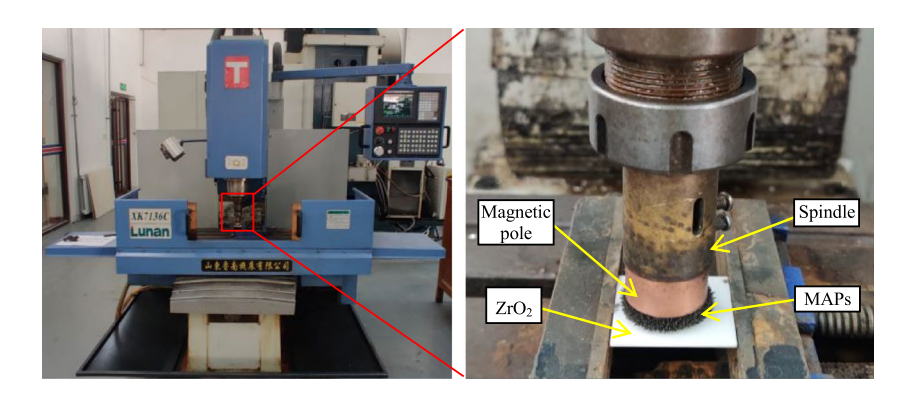
3.3 Surface integrity measurements

During the experiment, a super depth of field microscope (DSX1000) was used to observe the 2D morphological changes of ZrO₂ surface and subsurface. The 3D morphological changes of ZrO₂ surface were observed by a white light interferometer (MicroXAM-100). The surface roughness Ra and material removal amount MR of ZrO₂ surface were measured by a roughness meter (NDT150) and a precision electronic balance (HC5003), respectively. The grinding pressure of MAPs on the ZrO₂ surface was measured by a dynamometer (Kistler9257B). The temperature and residual stress on the ZrO₂ surface were analyzed by a thermal imager (UTi260B) and a X-ray stress analyzer (3000 G2R), respectively. To reduce measurement errors, the surface roughness Ra and residual stress for each group of experiment are averaged at multiple points.

4 Results and discussion

4.1 Surface morphology and surface roughness

Figure 5 shows the surface morphology of ZrO₂ under different machining gaps and the morphology changes of





magnetic abrasive brush adsorbed by the magnetic pole before and after grinding. It can be seen that the original surface quality of ZrO2 is poor, with a large number of scratches of varying depths. The MAPs adsorbed by the magnetic pole is orderly distributed along the magnetic field line (Fig. 5a). When the machining gap is 3 mm, deep scratches begin to become shallow, with almost no pits generated, but there are still many scratches. The MAPs adsorbed by the magnetic pole has a compression deformation trend (Fig. 5b). At this time, the grinding gap is large, the magnetic field strength in the machining area is low, the grinding pressure is small, and the number of MAPs involved in grinding is small. During the grinding process, the ceramic surface changes mainly due to plastic deformation. When the machining gap is reduced to 2.5 mm, the scratches on the workpiece surface become further shallower, with occasional pits appearing. After grinding, the MAPs adsorbed by the magnetic pole is significantly compressed (Fig. 5c), and more MAPs is involved in the grinding process. At this time, the ZrO₂ surface begins to exhibit plastic removal.

When the machining gap is reduced to 2 mm, the scratches on the ZrO₂ surface are basically removed, with a few pits generated, and the surface integrity is the best. After grinding, the MAPs adsorbed by the magnetic pole is further compressed, with a flat and uniform overall shape (Fig. 5d). At the same time, the number of MAPs participating in the grinding is almost maximized. The magnetic abrasive brush still mainly maintains flexible processing, and the rolling fluidity and self-renewal efficiency of MAPs are high. The ZrO₂ surface is mainly plastic removal. When the machining gap decreases to 1.5 mm, the number of pits on the ceramic surface begins to increase, and the surface integrity deteriorates. After grinding, part of the MAPs adsorbed by the magnetic pole is extruded from the machining area (Fig. 5e). This is because the gap is relatively small, and the magnetic abrasive brush begins to transition from flexible to rigid. The extrusion force between the MAPs increases, and the grinding pressure further increases. Some MAPs begins to roll hard, and the grinding performance of MAPs decreases. At this time, the removal method begins to transform from plastic removal to brittle removal. When the machining gap decreases to 1 mm, the number of pits on the surface of the workpiece further increases, and a large number of cracks appear. The integrity of the ceramic surface becomes worse. After grinding, more MAPs adsorbed by the magnetic pole is squeezed out of the machining area, and the amount of remaining MAPs on the surface of the magnetic pole is small (Fig. 5f). This is because when the machining gap is small enough, the magnetic abrasive brush is almost rigid, the extrusion pressure between the MAPs is large, and the fluidity of the MAPs is poor. At the same time, a large number of MAPs are squeezed out of the machining area, resulting in a small number of effective MAPs participating in the grinding process. It is difficult to renovate the MAPs, and the machining performance of the MAPs decreases sharply. The main method of ZrO₂ surface removal is brittle removal.

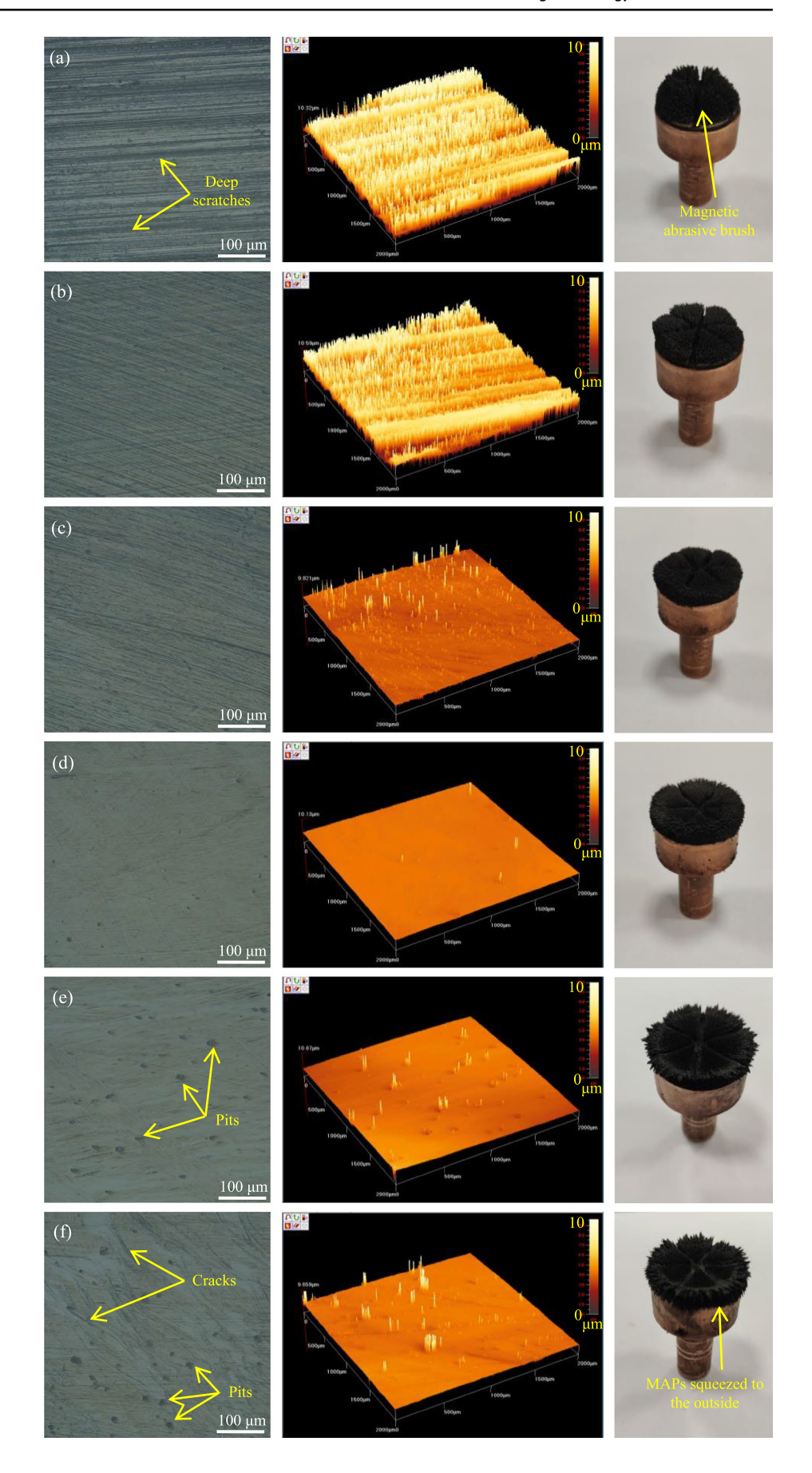
Figure 6 shows the changes in surface roughness Ra and material removal amount MR of ZrO2 under different machining gaps. As the machining gap decreases, the ZrO₂ surface roughness Ra first decreases and then increases, and the material removal amount MR first increases and then decreases. When the gap is large (3 mm), the Ra of ZrO₂ decreases slowly, and the MR basically does not change. This is because the grinding pressure is low at this time, and the number of MAPs involved in grinding is small. The CBN abrasives mainly scratch and press the ZrO2 surface without cutting. The ceramic surface only undergoes plastic deformation and almost no material removal. When the gap is 2.5 mm, the Ra decreases significantly, and the the MR begins to increase. At this time, the number of MAPs participating in grinding rapidly increases, and the grinding pressure increases, and the ZrO₂ surface is removed by plastic cutting with MAPs. The Ra further decreases, and the MR further increases, with the gap reducing to 2 mm. The average Ra is as low as 0.051 µm, and the MR reaches 19 mg within 10 min. At this time, the gap is moderate, and the number of MAPs participating in grinding is maximized. The MAPs fully contact the workpiece surface, resulting in high grinding pressure, good fluidity of the MAPs, and more prominent replacement. The ZrO2 surface is still primarily plastic removed, with a minimum surface roughness. As the gap continues to decrease, the Ra increases and the MR decreases rapidly. At this time, although the grinding pressure increases, the number of MAPs participating in the grinding rapidly decreases. Meanwhile, the flexible grinding brush begins to transition from plastic to rigid, the material removal method gradually shifts towards brittle removal, and the self-renewal and rolling degree of the MAPs become worse, which in turn reduces the processing efficiency and quality of MAPs.

4.2 Grinding force

Figures 7 and 8 show the grinding pressure changes of MAPs on ZrO₂ under different machining gaps. As the gap decreases, the grinding pressure increases. When the gap decreases from 3 to 1 mm, the average grinding pressure increases from 1.27 N to 10.28 N. As can be seen from Fig. 7, as the machining gap decreases, the grinding pressure increases while its fluctuations gradually increase, and the grinding force becomes increasingly unstable. This is because as the gap decreases, the magnetic abrasive brush gradually changes from flexible to rigid, resulting in lower fluidity and self-renewal efficiency of MAPs. The CBN abrasives cannot be timely updated after being blunt, which prevents the grinding process from being in a relatively stable



Fig. 5 2D and 3D surface morphology of ZrO₂ and morphology of magnetic abrasive brush under different machining gaps: (a) Original, (b) 3 mm, (c) 2.5 mm, (d) 2 mm, (e) 1.5 mm, (f) 1 mm





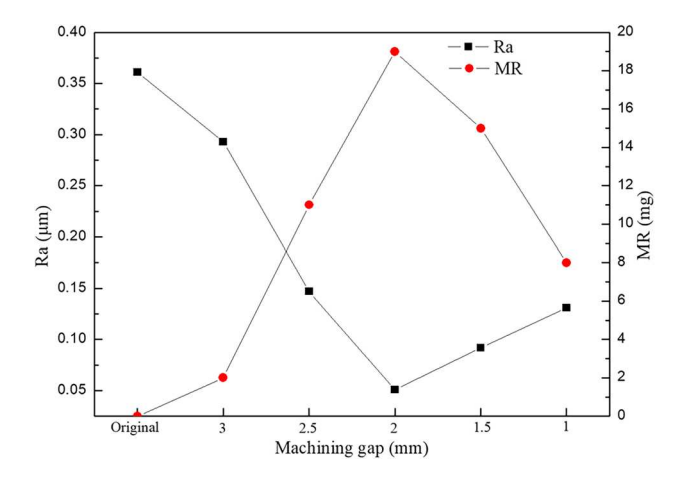


Fig. 6 Surface roughness Ra and material removal amount MR of ZrO₂ under different machining gaps

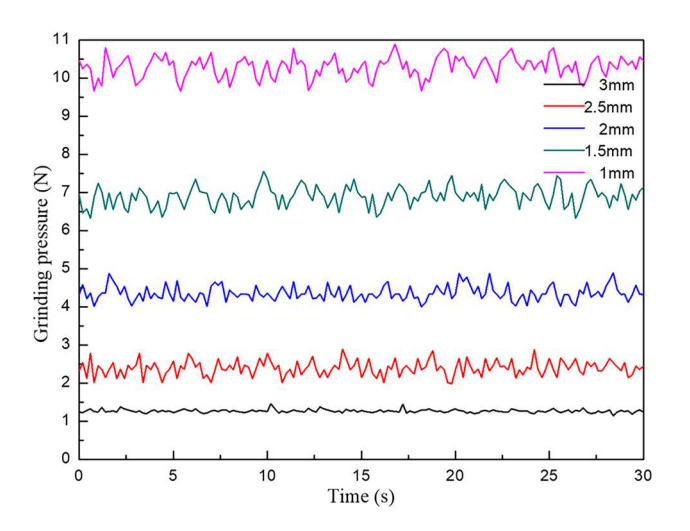


Fig. 7 Grinding pressure changes of MAPs on ${\rm ZrO}_2$ under different machining gaps

state. Moreover, as the gap decreases, the MAPs is gradually squeezed out of the machining area, and the MAPs adsorbed by the magnetic pole also begins to become uneven, resulting in inhomogeneous grinding pressure. On the other hand, with the decrease of gap and the increase of grinding pressure, the mode of ceramic surface removal begins to transform from plastic removal to brittle removal. During the brittle removal process, the sudden change in grinding force caused by the fracture and breakage of ceramic materials is also an important factor that leads to unstable changes in grinding force. Therefore, when selecting the machining gap, it is necessary to consider its stability while ensuring a large grinding pressure, so as to ensure a more uniform surface integrity of the workpiece in MAF.

As can be seen from Fig. 8, the rate of change of the average grinding pressure gradually increases as the machining

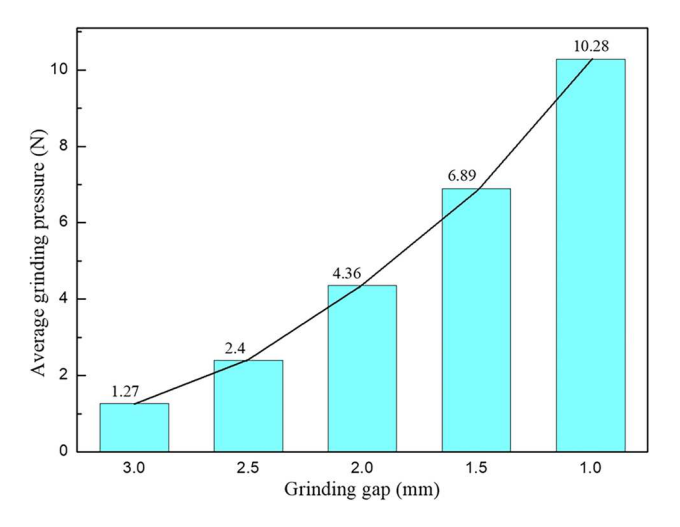


Fig. 8 Average grinding pressure of MAPs on ${\rm ZrO_2}$ under different machining gaps

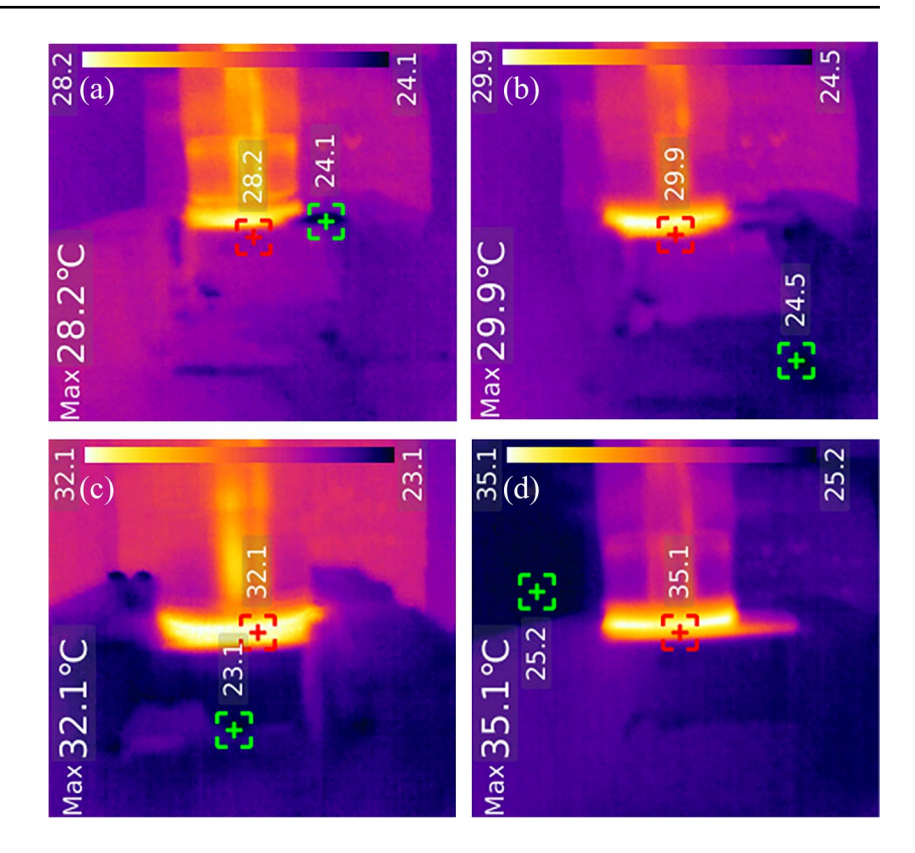
gap decreases. The grinding pressure F of a single MAP on the ZrO2 surface is caused by the combined action of the magnetic force F_1 generated by the magnetic pole, the magnetic traction force F_2 and the extrusion force F_3 of the surrounding MAPs. As the gap decreases, although the magnetic field becomes larger, the number of MAPs in the machining area gradually decreases, resulting in a gradual reduction in the total magnetic force ΣF_1 and the total magnetic traction force ΣF_2 of the MAPs participating in the grinding process. However, the growth rate of the total grinding pressure ΣF is an upward trend. This indicates that when the machining gap is small enough, the grinding pressure is mainly determined by the total extrusion force ΣF_3 of the magnetic pole to the MAPs. Therefore, when the machining gap is small, the mutual extrusion pressure between MAPs is relatively large, and the tumbling and fluidity of the MAPs become poor, resulting in unstable grinding pressure and bad surface integrity of ZrO₂.

4.3 Surface temperature and residual stress

Figure 9 shows the surface temperature changes of ZrO₂ under different machining gaps. It can be seen that the surface temperature increases slightly with the decrease of the machining gap. When the gap decreases from 2.5 mm to 1 mm, the maximum surface temperature of ZrO₂ increases from 28 °C to 35 °C, only increasing by about 7 °C. In this experiment, there are three main reasons why the machining gap has little impact on temperature. First, although the grinding pressure gradually increases as the machining gap decreases, the number of MAPs involved in grinding gradually decreases, and the total heat generated by grinding does not vary significantly. Secondly, the MAPs used in this test is the spherical CBN MAPs prepared by gas atomization.



Fig. 9 Surface temperature of ZrO₂ under different machining gaps: (a) 2.5 mm, (b) 2 mm, (c) 1.5 mm, (d) 1 mm



During the grinding process, the fluidity and replacement efficiency of the MAPs are high, and heat is not easily accumulated. In addition, the abrasive phase is CBN ceramic, with good thermal conductivity. Finally, in order to ensure the grinding quality, the quantitative water-based grinding fluid added in each group of experiments also takes away some of the heat generated in MAF.

Figure 10 shows the average residual stress changes on the surface of ZrO_2 under different machining gaps. In practical applications, the generation of compressive stress can greatly enhance the creep and fatigue resistance of ZrO_2 , thereby improving the performance and fatigue life of the workpiece. In the process of grinding ZrO_2 , the residual stress in the ceramic surface layer is mainly caused by two aspects: cold plastic deformation caused by grinding pressure and hot plastic deformation caused by grinding heat. As can be seen from the above, the temperature in MAF is not high, and as the machining gap decreases, the temperature changes little, resulting in little grinding heat. Therefore, the main reason that affects the change in residual stress on the ZrO_2 surface in this experiment is caused by the change in grinding pressure.

As can be seen from Fig. 10, with the reduction of machining gap, the residual compressive stress on the ZrO_2 surface first increases then decreases. When the gap is 3 mm, the residual stress on the workpiece surface does not change much, because the grinding pressure is small at this time, and the plastic deformation effect of MAPs on

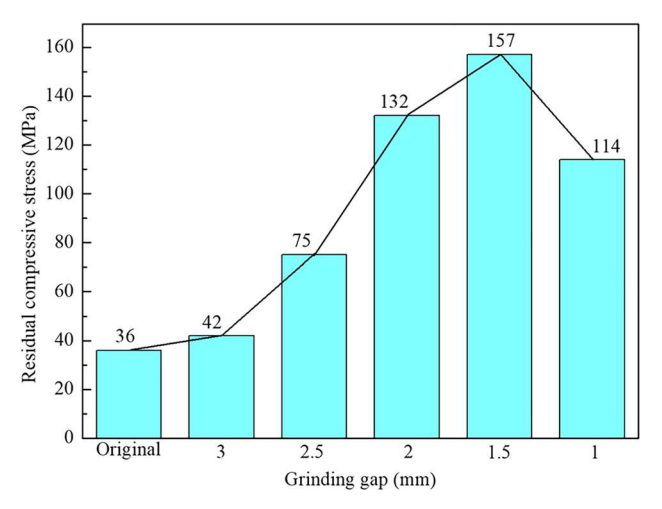
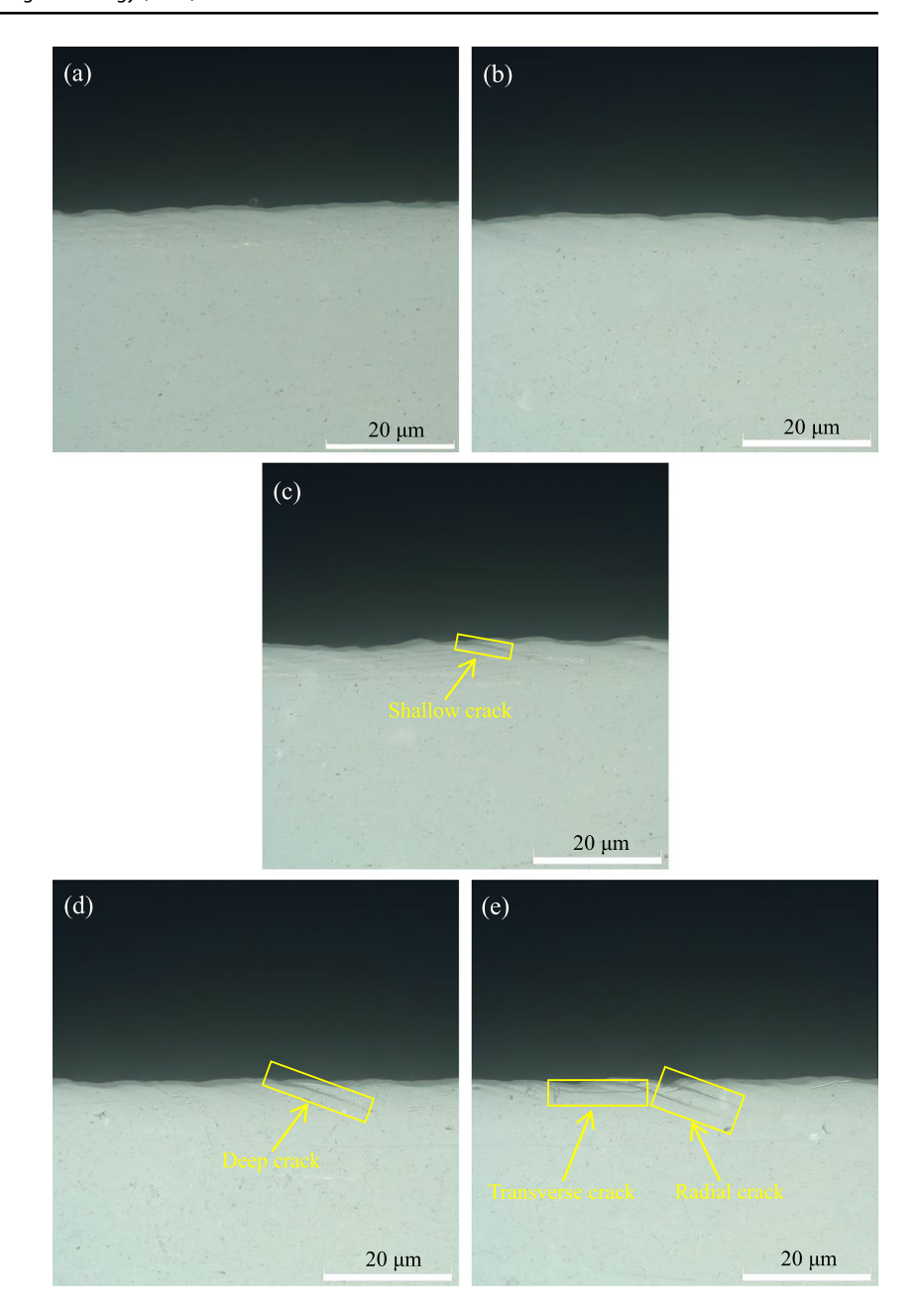


Fig. 10 Residual stress on the surface of ZrO₂ under different machining gaps

the ceramic surface is not obvious. When the gap decreases to 2.5 mm and 2 mm, the residual compressive stress on the ceramic surface increases significantly. At this time, the grinding pressure is relatively high, and more MAPs participate in the grinding process. The material removal is mainly plastic deformation removal. After micro cutting and repeated pressing by the MAPs, the residual compressive stress on the $\rm ZrO_2$ surface continues to increase. When the gap decreases to 1.5 mm, the residual compressive



Fig. 11 Subsurface morphology of ZrO₂ under different machining gaps: (a) 3 mm, (b) 2.5 mm, (c) 2 mm, (d) 1.5 mm, (e) 1 mm



stress still increases, but the increasing trend is significantly slower. This is because although the grinding pressure continues to increase, the number of MAPs involved in grinding begins to decrease, and the removal method of ceramic materials begins to transform from plastic deformation removal to brittle fracture removal, causing pits and microcracks on the ceramic surface, resulting in the generation of residual tensile stress. When the gap decreases to 1 mm, the average residual compressive stress decreases instead. This is because the main method of ceramic material removal at this time is brittle removal, resulting in a large number of pits and cracks on the ceramic surface, and the residual tensile stress component gradually increases,

thereby reducing the average residual compressive stress on the ZrO_2 surface.

4.4 Subsurface damage

Figure 11 shows the subsurface morphology of ZrO_2 under different machining gaps. It was observed that no microcracks were found on the subsurface of ZrO_2 when the machining gap was 3 mm and 2.5 mm (Fig. 11a and 11b). At this time, the machining gap is large, and the magnetic field intensity in the machining area is small. The grinding pressure F generated by MAPs on the ZrO_2 surface is smaller than the critical load F_R that causes radial cracks on



the ${\rm ZrO_2}$ subsurface. CBN MAPs perform plastic grinding on the ${\rm ZrO_2}$ surface. When the machining gap is 2 mm, it is observed that a very small amount of shallow radial microcracks occur on the ${\rm ZrO_2}$ subsurface (Fig. 11c). Although plastic grinding is still the main method at this time, as the gap decreases, the grinding pressure increases and the pressure fluctuation also increases. Therefore, few MAPs will cause the grinding pressure on the ceramic surface to break through the critical load of radial cracks, making $F > F_R$, and a small amount of radial microcracks will begin to appear.

When the machining gap decreases to 1.5 mm, the cracks on the ZrO₂ subsurface significantly deepen (Fig. 11d). At this time, the grinding pressure further increases, and more MAPs generate a grinding pressure on the ZrO₂ surface that is higher than the critical load for radial crack. The grinding way of ZrO₂ by MAPs begins to transition from plastic grinding to brittle grinding. When the machining gap is reduced to 1 mm, the number of radial cracks increases significantly, accompanied by transverse cracks (Fig. 11e). At this time, because the machining gap is small enough, the grinding pressure generated by MAPs on the ZrO2 surface is large (Figs. 7 and 8), and the number of MAPs in the machining area is small (Fig. 5f), so the grinding pressure generated by a single MAP on the ceramic surface is even greater. The grinding pressure generated by multiple MAPs participating in MAF on the ceramic surface is higher than the critical load F_R of the radial crack, resulting in radial cracks. At the same time, there are also some MAPs that generate transverse cracks on the ceramic subsurface due to the grinding pressure higher than the critical load F_T of transverse crack. At this time, most CBN MAPs remove ZrO₂ surface mainly through brittle removal in MAF.

5 Conclusions

In this study, spherical CBN/Fe-based MAPs prepared by gas atomization were used to grind ZrO₂ by MAF under different machining gaps. The effects of machining gap on the surface integrity of ZrO₂ were analyzed. The conclusions are as follows:

1. In MAF, the grinding pressure F of MAPs on ZrO_2 is mainly generated by the magnetic force F_1 generated by the magnetic pole, the magnetic traction force F_2 and the extrusion force F_3 between MAPs. As the machining gap decreases, the grinding pressure F gradually increases. When the gap is large, the magnetic field strength in the machining area is weak, resulting in small grinding pressure, as well as little pressure fluctuation. When the gap is moderate, the grinding pressure F is mainly generated by the magnetic force F_1 and the magnetic traction force

- F_2 . When the gap is small, the magnetic abrasive brush changes from flexible to rigid, and the pressure fluctuation changes greatly. The grinding pressure F is mainly generated by the extrusion force F_3 .
- 2. During the grinding process, when the machining gap is large, the number of MAPs involved in grinding is small, and the ZrO₂ surface is mainly plastic deformation, with almost no change in roughness Ra and material removal MR. When the gap is moderate, the number of MAPs involved in grinding is maximized. The magnetic abrasive brush performs plastic removal of the ZrO₂ surface in a flexible state, resulting in a rapid reduction in Ra, a rapid increase in MR, and the best surface integrity of the workpiece. When the gap is small, the number of MAPs in the machining area decreases rapidly, and the ZrO₂ surface is mainly subject to brittle removal. Surface cracks and pits increase, resulting in an increase in Ra, a reduction in MR, and poorer surface integrity.
- 3. In this experiment, the machining gap has little effect on the temperature change of the ZrO₂ surface, and the residual stress change is mainly affected by the grinding pressure. When the machining gap is large, the grinding pressure is small and the residual stress changes little. As the machining gap decreases, the grinding pressure increases, and the ZrO₂ surface is mainly plastic removed. After repeated cutting and extrusion of CBN MAPs, the residual compressive stress rapidly increases. When the machining gap is smaller, the grinding pressure is high, and the ceramic surface is mainly brittle removed, causing tensile stress on the ZrO₂ surface.
- 4. Small machining gaps can cause subsurface damage to ZrO₂. As the machining gap decreases, the grinding pressure increases and the number of MAPs participating in the grinding decreases, resulting in a large grinding pressure on the ZrO₂ surface by a single MAP which exceeds the critical load for generating radial and transverse cracks. Cracks begin to appear on the ZrO₂ subsurface. Therefore, appropriate machining gap can prevent the subsurface damage of ZrO₂ in MAF. The optimal machining gap in this experiment is 2 mm.

Author contributions Linzhi Jiang contributed to the investigation, conduction of MAF experiments and writing of the original draft, writing of the review, and editing.

Tieyan Chang, Guixiang Zhang and Yu-Sheng Chen contributed to the writing of the review, editing, and funding acquisition.

Xue Liu and Haozhe Zhang contributed to the review and editing with the order provided.

Funding This work is supported by the National Natural Science Foundation of China (No. 52275448). NSF's ChemMatCARS, Sector 15 at the Advanced Photon Source, Argonne National Laboratory



is supported by the Divisions of Chemistry and Materials Research, National Science Foundation, under grant number NSF/CHE-1834750.

Declarations

Ethics approval Not applicable.

Consent to participate The manuscript has been read and approved by all named authors.

Consent to publish All the authors listed in the manuscript have approved the manuscript will be considered for publication in The International Journal of Advanced Manufacturing Technology.

Competing interests The authors declare no competing interests.

References

- Sun J, Xie B, Zhu Z (2023) Extrusion-based 3D printing of fully dense zirconia ceramics for dental restorations. J Eur Ceram Soc 43:1168–1177. https://doi.org/10.1016/j.jeurceramsoc.2022.10. 076
- Yang M, Li C, Zhang Y, Jia D, Zhang X, Hou Y, Li R, Wang J (2017) Maximum undeformed equivalent chip thickness for ductile-brittle transition of zirconia ceramics under different lubrication conditions. Int J Mach Tool Manufact 122:55–65. https://doi.org/10.1016/j.iimachtools.2017.06.003
- Zhu L, Xu Y, Liu S, Chen H, Tao J, Tong X, Li Y, Ma J (2023) Microstructure, mechanical properties, friction and wear performance, and cytotoxicity of additively manufactured zirconiatoughened alumina for dental applications. Compos Part B-Eng 250:110459. https://doi.org/10.1016/j.compositesb.2022.110459
- Wang Y, Lam W, Luk H, Shih K, Botelho M (2020) The adverse effects of tungsten carbide grinding on the strength of dental zirconia. Dent Mater 36:560–569. https://doi.org/10.1016/j.dental. 2020.02.002
- Lai X, Si W, Jiang D, Deng B (2017) Effects of small-grit grinding and glazing on mechanical behaviors and ageing resistance of a super-translucent dental zirconia. J Dent 66:23–31. https://doi.org/ 10.1016/j.jdent.2017.09.003
- Deng X, Zhang F, Zhou Y (2022) Effect of grinding parameters on surface integrity and flexural strength of 3Y-TZP ceramic. J Eur Ceram Soc 42:1635–1644. https://doi.org/10.1016/j.jeurcerams oc.2021.12.018
- Tang H, Deng Z, Guo Y (2015) Depth-of-cut errors in ELID surface grinding of zirconia-based ceramics. Int J Mach Tool Manufact 88:34–41. https://doi.org/10.1016/j.ijmachtools.2014.08.003
- Minguela J, Ginebra M, Llanes L, Mas-Moruno C, Roa J (2020) Influence of grinding/polishing on the mechanical, phase stability and cell adhesion properties of yttria-stabilized zirconia. J Eur Ceram Soc 40:4304–4314. https://doi.org/10.1016/j.jeurcerams oc.2020.03.049
- Wan L, Li L, Deng Z, Liu W (2019) Thermal-mechanical coupling simulation and experimental research on the grinding of zirconia ceramics. J Manuf Process 47:41–51. https://doi.org/10.1016/j. jmapro.2019.09.024
- Denkena B, Wippermann A, Busemann S, Kuntz M, Gottwik L (2018) Comparison of residual strength behavior after indentation, scratching and grinding of zirconia-based ceramics for medicaltechnical applications. J Eur Ceram Soc 38:1760–1768. https:// doi.org/10.1016/j.jeurceramsoc.2017.11.042

- Ma Z, Wang Q, Chen H, Chen L, Qu S, Wang Z (2022) A grinding force predictive model and experimental validation for the laser-assisted grinding (LAG) process of zirconia ceramic. J Mater Process Tech 302:117492. https://doi.org/10.1016/j.jmatprotec. 2022.117492
- Liu W, Tang D, Gu H, Wan L (2022) Experimental study on the mechanism of strain rate on grinding damage of zirconia ceramics. Ceram Int 48:21648–21655. https://doi.org/10.1016/j.ceram int 2022 04 142
- Zhang X, Wang Z, Shi Z, Jiang R (2020) Improved grinding performance of zirconia ceramic using an innovative biomimetic fractal-branched grinding wheel inspired by leaf vein. Ceram Int 46:22954–22963. https://doi.org/10.1016/j.ceramint.2020.06.070
- Xiao X, Zheng K, Liao W, Meng H (2016) Study on cutting force model in ultrasonic vibration assisted side grinding of zirconia ceramics. Int J Mach Tool Manufact 104:58–67. https://doi.org/ 10.1016/j.ijmachtools.2016.01.004
- Yamaguchi H, Kang J, Hashimoto F (2011) Metastable austenitic stainless steel tool for magnetic abrasive finishing. CIRP Ann-Manuf Techn 60:339–342. https://doi.org/10.1016/j.cirp.2011.03. 119
- Zhang G, Zhao Y, Zhao D, Yin F (2011) Preparation of white alumina spherical composite magnetic abrasive by gas atomization and rapid solidification. Scripta Mater 65:416–419. https:// doi.org/10.1016/j.scriptamat.2011.05.021
- Jiang L, Chang T, Zhu P, Zhang G (2021) Influence of process conditions on preparation of CBN/Fe-based spherical magnetic abrasive via gas atomization. Ceram Int 47:31367–31374. https:// doi.org/10.1016/j.apt.2020.01.036
- Jiang L, Chang T, Zhang G, Zhao Y (2022) Formation mechanism of ceramic/metal composite spherical magnetic abrasive prepared via gas-solid atomization. J Alloy Compd 923:166400. https://doi. org/10.1016/j.jallcom.2022.166400
- Heng L, Kim J, Tu J, Mun S (2020) Fabrication of precision meso-scale diameter ZrO₂ ceramic bars using new magnetic pole designs in ultra-precision magnetic abrasive finishing. Ceram Int 46:17335–17346. https://doi.org/10.1016/j.ceram int.2020.04.022
- Wang Y, Hu D (2005) Study on the inner surface finishing of tubing by magnetic abrasive finishing. Int J Mach Tool Manufact 45:43–49. https://doi.org/10.1016/j.ijmachtools.2004.06.014
- 21. Zhang Y (1988) Metal cutting theory. Aviation Industry Press, Beijing
- Lawn B, Evans A (1977) A model for crack initiation in elastic/ plastic indentation fields. J Mater Sci 12:2195–2199
- Deng C, Zhang B, Sun Z (2002) Research progress on the removal mechanism of ceramic grinding materials. Chin J Mech Eng 18:84–87. https://kns.cnki.net/kcms2/article/abstract?v=3uoqI hG8C44YLTlOAiTRKgchrJ08w1e7lwLRIsgSA98QLyhrv5Vvvj5 WRpCf_aOeb9horfszjJpmSM0Be8NOW-NhhvxCxRkw&unipl atform=NZKPT

Publisher's Note Springer Nature remains neutral with regard to jurisdictional claims in published maps and institutional affiliations.

Springer Nature or its licensor (e.g. a society or other partner) holds exclusive rights to this article under a publishing agreement with the author(s) or other rightsholder(s); author self-archiving of the accepted manuscript version of this article is solely governed by the terms of such publishing agreement and applicable law.

